

# Giant coherence in driven systems

Soumen Roy<sup>\*</sup>, Debasis Dan<sup>+</sup> and A. M. Jayannavar<sup>†</sup>

<sup>\*</sup>,<sup>†</sup> Institute of Physics, Bhubaneswar 751005, India

<sup>+</sup> Dept. of Biology and Center for Genomics and Bioinformatics, Indiana University, Bloomington 47405 USA

E-mail: <sup>\*</sup> [sroy@iopb.res.in](mailto:sroy@iopb.res.in), <sup>+</sup> [ddan@indiana.edu](mailto:ddan@indiana.edu), <sup>†</sup> [jayan@iopb.res.in](mailto:jayan@iopb.res.in)

## Abstract.

We study the noise-induced currents and reliability or coherence of transport in two different classes of rocking ratchets. For this, we consider the motion of Brownian particles in the over damped limit in both adiabatic and non-adiabatic regimes subjected to unbiased temporally symmetric and asymmetric periodic driving force. In the case of a time asymmetric driving, we find that even in the presence of a spatially symmetric simple sinusoidal potential, highly coherent transport occurs. These ratchet systems exhibit giant coherence of transport in the regime of parameter space where unidirectional currents in the deterministic case are observed. Outside this parameter range, i.e., when current vanishes in the deterministic regime, coherence in transport is very low. The transport coherence decreases as a function of temperature and is a non-monotonic function of the amplitude of driving. The transport becomes unreliable as we go from the adiabatic to the non-adiabatic domain of operation.

PACS numbers: 05.40.Jc, 05.40.Ca, 02.50.Ey

**Keywords:** Brownian motion, stochastic particle dynamics (Theory), transport processes / heat transfer (Theory)

## 1. Introduction

Ratchets, Brownian motors or rectifiers are nonequilibrium systems that rectify fluctuations in the medium to achieve directed motion [1, 2, 3, 4, 5]. The main criteria for these systems are spatially extended periodic structures and unbiased external fluctuations that drive the system out of equilibrium. Preferential directed motion is possible if either the potential and/or the external fluctuations is asymmetric (broken symmetry) [1]. Even in the presence of a spatially asymmetric potential, the principle of detailed balance prohibits any net unidirectional current at equilibrium. Only when the system is driven out of equilibrium, this principle no longer holds and the Brownian particles can achieve directed motion by rectification of thermal fluctuations. These *ratchet models* are found to have wide ranging applications in physical and biological systems [1, 2, 3, 4, 5].

Considerable amount of work has been devoted to understand the nature of currents and their reversals in different classes of ratchet models (namely flashing ratchets [2], rocking ratchets [6], frictional ratchets [7], etc). Moreover, these ratchets or motors are engines at the molecular scale converting input energy from a nonequilibrium environment into useful work. Hence a lot of attention has been given to the performance characteristics of these systems, namely thermodynamic [8, 9, 10, 11] and generalised [12, 13] efficiencies. In recent years, another important property of these systems is being explored, namely the reliability or coherence of transport.

The unidirectional current of Brownian particles in stochastic ratchets, however, is always accompanied by a diffusive spread (dispersion). This spread is intimately related to the question of reliability or quality of transport to the extent that it may completely overshadow the ratcheting effect in a system with finite spatial extensions. For example, if a particle on an average moves a distance  $L$  due to its finite average velocity,  $v$ , there will always be an accompanying diffusive spread. If this spread is much smaller than the distance traveled, then the motion of the particle is considered as coherent or reliable. This, in turn, can be quantified in terms of a dimensionless number called the Péclet number ( $Pe$ ), which is the ratio of the average velocity,  $v$ , to the diffusion constant,  $D$ . More specifically  $Pe = vL/D$ . In our studies, we take  $L$  to be the length of the period of the relevant spatially periodic potential. Quantitatively, if  $Pe \gg 2$ , the transport is said to be coherent, otherwise it is incoherent or unreliable. There exist very few studies, which address the question of reliability of transport.  $Pe$  for some models of flashing and rocking ratchets were found to be  $\sim 0.2$  and  $\sim 0.6$  respectively [14], implying a less reliable transport. A study on symmetric periodic potentials along with a spatially modulated white noise showed a coherent transport with  $Pe$  less than 3. In the same study a special kind of strongly asymmetric potential was found to increase  $Pe$  to 20 in some range of physical parameters [15, 16]. Experimental studies in biological motors show them to exhibit highly efficient and reliable transport with  $Pe$  ranging from 2 to 6 [17]. In a very recent work, the collective effects of coupled Brownian motors were found to show high transport coherence [18]. Reliability of transport has also

been studied in frictional ratchets and coherent transport is observed in a part of the parameter space [19].

In the present work, we study the transport coherence in two different classes of rocking ratchets. In the first case (hereafter referred to as *case 1*), we study a ratchet model, where the potential is simply sinusoidal (spatially symmetric) while the driving is temporally asymmetric. In Refs. [20, 21, 22] an unbiased discontinuous temporally asymmetric driving has been considered. For the case of the asymmetric drive, characterised by an additive Poissonian white shot noise with a constant bias ensuring zero time average, analytical solutions have been obtained for the noise induced currents [23]. The time asymmetric drive can be generated by the application of biharmonic drive at frequencies  $\omega$  and  $2\omega$ . This phenomenon is known as harmonic mixing [24] and has been studied extensively in the context of ratchet dynamics [25], in the problem of kink-assisted directed energy transport in soliton systems [26] etc. Experimentally time asymmetric ratchet mechanism has been used to generate photocurrent in semiconductors [27] (for details see section 5.2 of Ref. [1]). Recently, Brownian motors with time-asymmetric driving in a periodic potential have been realised in cold atoms in a dissipative optical lattice [28]. In the second case (hereafter referred to as *case 2*), the ratchet is characterised by a spatially asymmetric potential driven by a temporally symmetric ac force. We report our results on the reliability of transport on the model earlier studied by Bartussek et al [29] in the same parameter space explored by them. Our work on transport coherence is relevant to the aforementioned experimental studies [3, 27, 28]. One can readily perform measurements of transport coherence in experimental set-ups akin to Ref. [28]. We show throughout this work that that these ratchets exhibit a *generic effect* in the deterministic limit (absence of noise or temperature) : if the ratchet exhibits a finite current, one observes giant coherence at low temperatures while if the current vanishes, the associated transport coherence is very low. Moreover, this enhanced coherence is maintained as long as currents in the backward direction are suppressed. The suppression of backward currents also leads to an enhanced thermodynamic efficiency of energy transduction [10, 11] in absence of which the thermodynamic efficiency in ratchet systems is very low [30]. The transport coherence decreases as a function of temperature and is a non-monotonic function of the driving amplitude. Moreover, the transport becomes less reliable as we approach the non-adiabatic domain of operation.

## 2. Model:

### 2.1. Case 1 : spatially symmetric potential with temporally asymmetric driving

The starting point of our equation is the Brownian motion of an overdamped particle in presence of a potential and a driving force which can be described by the overdamped Langevin equation [31].

$$\gamma\dot{x} = -\partial_x[V(x) - xF(t)] + \xi(t) \quad (1)$$

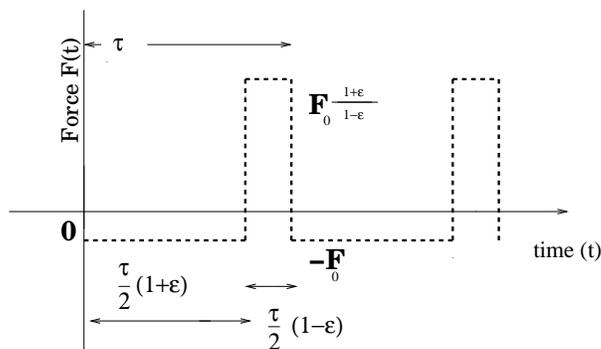


**Figure 1.** Illustration of time asymmetric force for time period  $\tau$  and temporal asymmetry factor  $\epsilon$

The thermal noise is modeled by a zero mean Gaussian white noise  $\xi(t)$ , with correlation  $\langle \xi(t)\xi(t') \rangle = 2k_B T \gamma \delta(t - t')$ . The periodic potential is chosen as  $V(x) = V_0 \sin(x)$ . Since  $V(x)$  is symmetric, to generate unidirectional currents, one has to apply a time asymmetric driving.  $F(t)$  is the externally applied time periodic driving force, whose average over a time period is zero [10, 20, 21] and is given by

$$F(t) = \frac{1 + \epsilon}{1 - \epsilon} F_0, \quad (n\tau \leq t < n\tau + \frac{1}{2}\tau(1 - \epsilon)), \quad (2)$$

$$= -F_0, \quad (n\tau + \frac{1}{2}\tau(1 - \epsilon) < t \leq (n + 1)\tau),$$

Here, the parameter  $\epsilon$  signifies the temporal asymmetry in the periodic forcing while  $\tau$  is the time-period and  $n = 0, 1, 2, \dots$  is an integer. The force profile is shown in Fig. 1.

### 2.2. Case 2 : spatially asymmetric potential with temporally symmetric driving

We consider the same ratchet model as considered by Bartussek et al [29] with the potential  $V(x) = -\frac{V_0}{k} [\sin(kx) + 0.25 \sin(2kx)]$  with  $k = 2\pi$ . We now impose a periodic unbiased ac force,  $F(t) = F_0 \sin(\omega t)$ . The underlying asymmetric potential breaks the symmetry of the system and generates a current .

## 3. Numerical details

The analytical expressions for the currents( $j$ ) and diffusion coefficient( $D$ ) can only be obtained in the adiabatic or quasi static limit , i.e., when the frequency of the driving force is small compared to the other frequency scales in the problem [10, 32]. In such a situation, the system can be considered to be in a steady state at each instant of time. For the general case, we are forced to take recourse to numerical simulations [33, 34]. In this work, we have used Langevin simulations to evaluate  $j$  and  $D$ . We use the Huen's method in these simulations[33] and calculate the current in the asymptotic regime. The expressions for  $j$  and  $D$  are given by,

$$j = \left\langle \frac{x(t) - x(t_0)}{t - t_0} \right\rangle \quad (3)$$

and

$$D = \lim_{t \rightarrow \infty} \frac{1}{2t} [\langle x^2(t) \rangle - \langle x(t) \rangle^2] \quad (4)$$

Here  $\langle \dots \rangle$  denotes ensemble averaging. We discard the initial transients ( $t_0 = 500\tau$ ) and then evolve the system for  $t = 25000\tau$ . In each case the time-step is taken equal to 0.01 and the averaging is done over 5000 ensembles.

In all the figures to follow, the physical quantities taken are in dimensionless units [16]. Energies are scaled with respect to the potential strength,  $V_0$ ; lengths are scaled with respect to the spatial period of the potential. Also, the frequency of oscillation is scaled with respect to the friction coefficient and  $F_0 \equiv \frac{FL}{V_0}$ . As a check we have reproduced the main results of Refs. [29, 35, 36]

## 4. Results and Discussion

### 4.1. case 1

Fig. 2 shows the variation of  $j$ ,  $D$  and  $Pe$  versus force. In our work, current( $j$ ) and velocity( $v$ ) carry the same meaning. We have taken the time period  $\tau = 1000$  to be very large so that we are in the quasi static limit. For a simple potential  $V(x) = V_0 \sin x$  in the presence of a static force ( $F_0$ ), in the deterministic limit current flows only when  $F_0$  crosses a critical threshold( $F_c$ ), namely,  $F_0 > F_c = 1$ . Beyond the critical threshold, barriers to the motion in the forward direction disappear. Consequently, the particle is in the running state (i.e., the particle is free to move). Below the critical field, the particle experiences barriers in the direction of the applied field and hence at temperatures  $T \rightarrow 0$ , particle will be trapped at a local minimum of the potential (i.e., in a locked state). It is also known that *giant diffusion* arises around the ‘‘dynamical bottleneck’’ at  $F_0 = F_c = 1$  and is expected as a fallout of the instability between the locked state and the running state [36, 37, 38]. The peaks in the  $D$  versus force curve around  $F_c \approx 1$ , gets sharpened as the temperature is reduced. At high temperatures, due to thermal smearing, the peaks become broader. In the adiabatic limit, we can consider the total current to arise from the sum of the contributions of the fraction of the current when the field is in the forward direction and the fraction of the current when the field is in the backward direction [19, 32]. In the same limit, we can also consider the total diffusion coefficient to arise from the sum of similar contributions of the diffusion coefficients from force fields in the forward and backward directions. As we increase the amplitude of the temporal force  $F_0$ , in the deterministic limit ( $T \rightarrow 0$  limit), current in the forward direction starts flowing when  $\frac{1+\epsilon}{1-\epsilon}F_0 > 1$  or  $F_0 > \frac{1-\epsilon}{1+\epsilon}$ . We have chosen  $\epsilon = 0.8$ , hence, one observes significant currents only above  $F_0 > 0.11$ . As we increase the amplitude  $F_0$ ,  $j$  increases till  $F_0$  becomes of the order of 1. Up to this limit, current in the backward direction is absent (as the force applied in the backward direction is  $F_0$  which is independent of  $\epsilon$ ). Thus in the range of  $F_0$  between  $\frac{1+\epsilon}{1-\epsilon}$  and 1, the current increases monotonically. Beyond  $F_0 > 1$  the barriers to motion for a particle in both

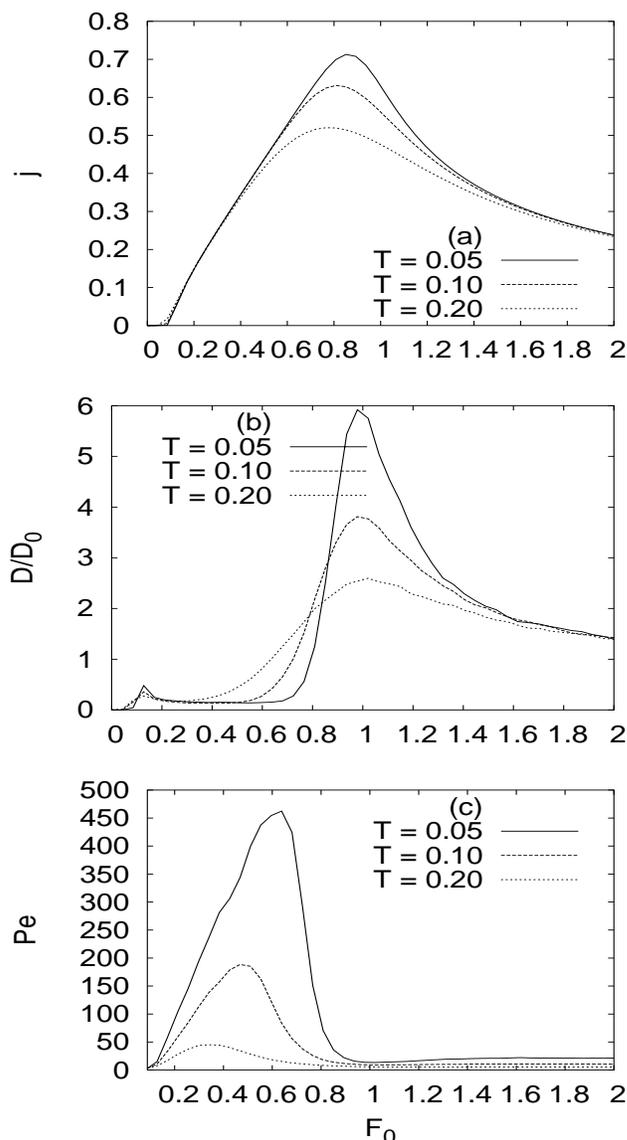


**Figure 2.** Plot of (a)  $j$  (b)  $D$  and (c)  $Pe$  (from above) versus  $F_0$  at  $\epsilon = 0.8$  for various values of  $T$  in the temporally asymmetric driving case in the adiabatic limit ( $\tau = 1000$ ).

directions disappear and consequently current decreases as we increase  $F_0$  further. The temperature only broadens the peak and the value of  $F_0$  at which the peak appears, shifts to the left. This is because, temperature can facilitate current in the backward direction, even when barriers are present.

In fig. 2(b), we have plotted  $D$  (scaled with respect to the bare diffusion coefficient,  $D_0 \equiv k_B T / \gamma$ ) versus the driving force  $F_0$ . For very small values of the driving force, i.e., when  $F_0 \ll 1$ ,  $D \ll D_0$  due to the presence of barriers in motion in both directions. Two peaks are observed at  $F_0 \approx 0.1$  and 1, which correspond to the vanishing of barriers for forward and backward directions respectively (i.e., instability points) as discussed earlier. The diffusion peak around  $F_0 = 1$  is pronounced and has a value greater than

1, i.e.,  $D \gg D_0$ . This is an anticipated effect [36, 37]. The peak broadens with the rise in temperature. However, unlike the peak in  $j$ , it does not shift with temperature [36].

We notice clearly from fig. 2(a) and fig. 2(b) that in the range between  $F_0 \approx 0.1$  and 1, *enhanced currents are accompanied by minimal diffusion*. As a consequence it is in this region, that one observes enhanced or giant transport coherence ( $Pe \approx 450$  for  $T = 0.05$  around  $F_0 \approx 0.6$ ). The observed values are very much larger than those obtained for other ratchet systems [14, 15, 16, 19]. It may be noted that, in the regime of giant coherence, current in the backward direction is suppressed as mentioned earlier. Precisely in this regime of  $F_0$ , it has been shown that the thermodynamic efficiency ( $\eta$ ) [10] and the generalised efficiency [39] is quite high, even though the ratchet operates in an irreversible mode.

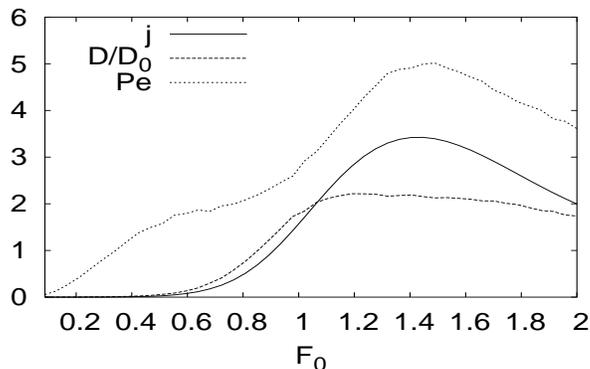


**Figure 3.** Plot of  $j$ ,  $D$  and  $Pe$  versus  $F_0$  at  $\epsilon = 0.8$  and  $\tau = 5$  (non-adiabatic limit) at  $T = 0.2$  in the temporally asymmetric driving case. The  $j$  has been scaled by a factor of 10.

We now very briefly discuss the nature of  $j$ ,  $D$  and  $Pe$  as a function of  $F_0$  in the non-adiabatic limit. For this, we have plotted in fig. 3 the variation of  $j$ ,  $D$  and  $Pe$  versus  $F_0$  for  $\tau = 5$  at  $T = 0.2$  and  $\epsilon = 0.8$ . We notice that  $j$  exhibits a peak shifted to the right as compared to the graph in the adiabatic limit i.e., fig. 2(a). The currents are very low for small  $F_0$ , even for the regime around ( $F_0 \geq 0.11$ ). In this regime, particle cannot take advantage of vanishing of barriers in the forward direction as it will not be able to traverse a distance of half a period in the duration in which the force is in positive direction, i.e., force reverses its sign before the particle could traverse a distance of half a period. However, on increasing the value of  $F_0$ , the particle will naturally take advantage of the vanishing barriers. Hence, peak shifts towards the right. Unlike adiabatic case,  $D$  does not exhibit a two-peak structure. The peak at smaller value of  $F_0 \approx 0.11$  disappears. Here too the particle does not take advantage of the vanishing of barriers in the forward motion.  $Pe$  exhibits values which are very much smaller than those obtained in the adiabatic limit. Hence, coherence in transport is reduced as the time-period is reduced.

Fig. 4 shows the variation of  $j$ ,  $D$ , and  $Pe$  with respect to  $T$  (scaled with respect to  $V_0$ , the strength of the potential) for various values of  $\epsilon$  at  $F_0 = 0.3$ . The  $j$  and  $D$

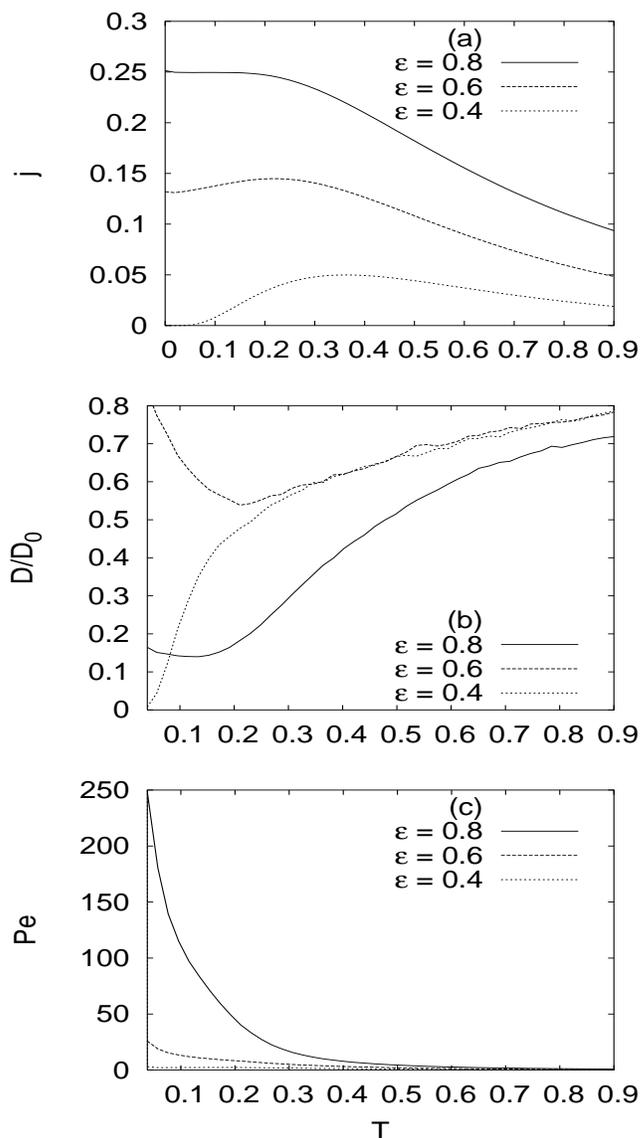


**Figure 4.** Plot of (a)  $j$  (b)  $D$  and (c)  $Pe$  (from above) versus  $T$  at  $F_0 = 0.3$  for various values of  $\epsilon$  in the temporally asymmetric driving case, in the adiabatic limit ( $\tau = 1000$ ).

versus  $T$  curves show the crucial role played by the temporal asymmetry factor  $\epsilon$ . The higher values of current are obtained for higher  $\epsilon$ . For  $\epsilon = 0.4$  at  $F_0 = 0.3$ , barriers for the motion of the particle are present in both the directions and as a result the current vanishes in the zero temperature limit. Thus, for intermediate values of temperature, a peak is witnessed. For other values of  $\epsilon$ , namely,  $\epsilon = 0.6$  and  $\epsilon = 0.8$ , barriers to the motion in the forward direction vanish but are present in the backward direction. Hence, at zero temperature, we get a finite current which vanishes at high temperature. For  $\epsilon = 0.8$  the current decreases monotonically whereas for  $\epsilon = 0.6$  the current exhibits a small peak.

The origin of the temperature axis in fig. 4(b) is at  $T = 0.04$ . The scaled

diffusion coefficient ( $D/D_0$ ) exhibits a minima as a function of temperature in the range considered (for  $\epsilon = 0.6, 0.8$ ). This is due to the fact that the scale  $D_0 \equiv k_B T / \gamma$ . We have observed that without this scaling factor,  $D$  increases monotonically with temperature, starting at zero at  $T = 0$ . In the high temperature limit,  $T > 1$ , (i.e., when  $T \gg V_0$ ),  $D/D_0 \rightarrow 1$  as anticipated. At low temperatures,  $D/D_0$  exhibits a non-monotonic behaviour as a function of  $\epsilon$ . Other quantities like the thermodynamic efficiency [10] and the generalised efficiency [39] also exhibit a non-monotonic behaviour as a function of the temporal asymmetry factor  $\epsilon$ . This is not surprising as there are two competing effects : as one increases  $\epsilon$ , the barriers in the forward direction are reduced while the fraction of the time period during which the particle is subject to a positive force is also decreased.

From fig. 4(c) we see that  $Pe$  diminishes as we increase the temperature. Higher the  $\epsilon$  value, higher is the coherence. This enhanced coherence is sustained over a large temperature regime. We would like to emphasise that at very low temperatures ( $T \rightarrow 0$ ), finite current results for a range of parameters. However,  $D$  tends to zero in the same range. As a result,  $Pe$  exhibits a divergent behaviour. Hence, to avoid numerical errors, the origin of the temperature axis is chosen as  $T = 0.04$ . It should be noted that for  $\epsilon = 0.4$ , current in the deterministic limit vanishes as can be observed in fig. 4(a) and consequently transport coherence is very low as seen from fig. 4(c). These results bring out the generic effect mentioned in Section 1.

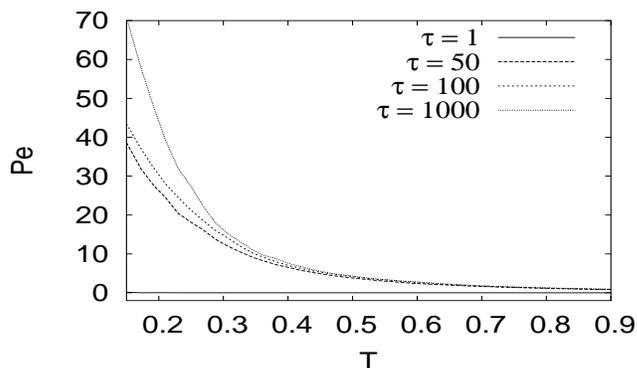


**Figure 5.** Plot of  $Pe$  versus  $T$  at  $\epsilon = 0.8$  and  $F_0 = 0.3$  for various values of the time period ( $\tau$ ) in the temporally asymmetric driving case.

In fig. 5, we show the variation of  $Pe$  for a fixed value of  $\epsilon = 0.8$ , as a function of time-period. The origin of the temperature axis is at  $T = 0.15$ . It is clear, that the transport which is coherent in the adiabatic limit ( $\tau = 1000$ ) loses its coherence as the non-adiabatic limit is reached. This conclusion about the superior reliability of transport of the ratchet at the adiabatic limit is generally true (we have verified this separately).

## 4.2. case 2

Now we turn to case 2, which has been studied extensively for the nature of currents by Bartussek et al [29]. In fig. 6, we have plotted  $D$  and  $Pe$  as a function of  $F_0$

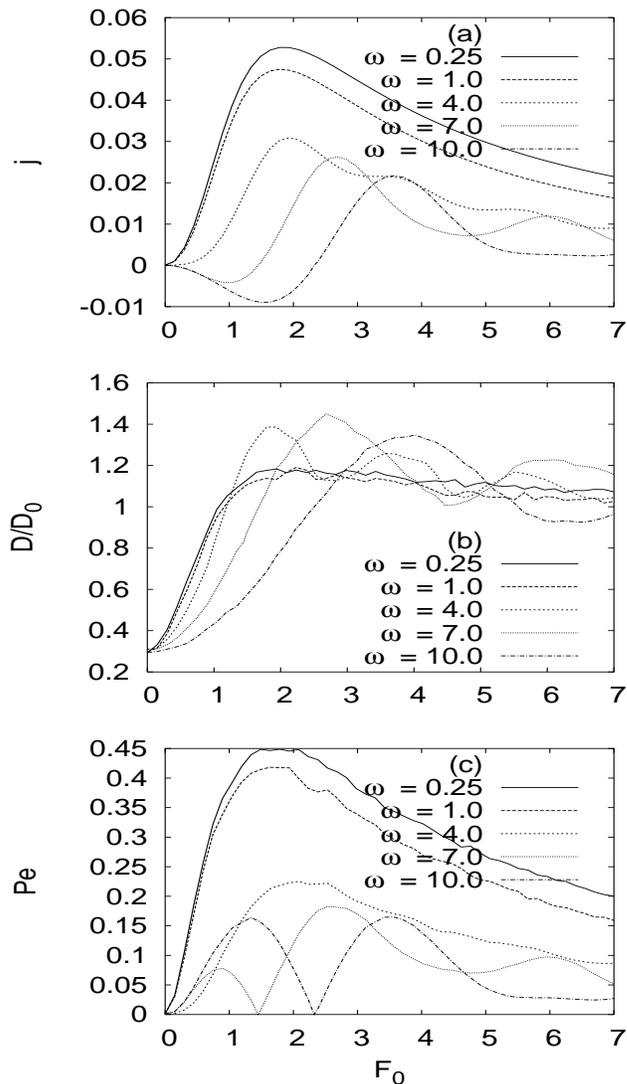


**Figure 6.** Plot of (a)  $j$  (b)  $D$  and (c)  $Pe$  (from above) versus  $F_0$  at  $T = 0.1$  for the temporally symmetric driving case.

at  $T = 0.1$  for various frequencies  $\omega$ . In fig. 6(a) we reproduce the same results as obtained in fig. 1(b) of Ref. [29].  $\omega = 0.25$  corresponds to the adiabatic regime. Here, current flows in a positive direction and exhibits a peak. During the fraction of the time-period when force is in positive direction, the particle experiences a smaller barrier in the forward direction as opposed to the fraction of the period when force is in the negative direction and particle experiences a higher potential barrier. During each half cycle particle traverses a distance much larger than the spatial period of the potential. In this regime, the particle takes advantage of the presence of anisotropy in the potential

and hence positive current arises [1]. As we approach the non-adiabatic limit ( $\omega = 7$ ,  $\omega = 10$ ), we observe multiple current reversals. For details see Refs. [29, 40].

In fig 6(b), we have plotted  $D$  as a function of  $F_0$  for various frequencies.  $D/D_0$  starts from a finite value at  $F = F_0$ , and asymptotically approaches 1 as expected. Some local maxima are observed at finite driving frequencies. These features are also seen for the case of symmetric periodic potential driven by a temporally symmetric periodic force as discussed in Refs. [35, 38]. These peaks are attributed to optimised enhancement of the escape rate by modulation for a given noise strength. As discussed in Refs. [35, 38], for certain values of the driving force (or forces), the position probability peak of the particles may just happen to be on the top of the potential barrier and the diffusion is naturally more than there would have been if this peak had been located elsewhere (especially if it was at the potential minimum for example).

In fig. 6(c) we have plotted corresponding  $Pe$  as a function of  $F_0$ . We readily notice that even in the adiabatic limit, transport is incoherent since values of  $Pe \approx 0.45$  are obtained which further decrease as we cross over to the non-adiabatic limit. Therefore the noise induced transport in this system is completely incoherent in the range of parameters considered here. *This range corresponds to the current being zero in the deterministic regime.*

We would like to emphasise that the phenomenon of current reversal in ratchets plays a major role in devising novel separation techniques for nanoparticles [4]. Once the current reversal as a function of any parameter is established, it follows readily that current reversals can be observed by varying other parameters in the system [1, 5]. In these devices, particles with different masses move in the opposite direction which can be readily separated. However, we notice from the figure that, around the current reversals, the Péclet numbers are quite small and transport is incoherent.

In fig. 7 we plot the variation of  $Pe$  as a function of  $F_0$  in the adiabatic limit ( $\omega = 0.25$ ) for two fixed values of  $T = 0.01$  and  $T = 0.1$ . The inset shows the variation of  $j$  as a function of  $F_0$  at  $T = 0.01$  and  $T = 0.1$ . At  $T = 0.01$ , we are close to the deterministic regime, where the values of  $j$  and  $Pe$  are expected to be large. The figure corresponding to  $T = 0.01$  shows a higher value of  $Pe$ . In the adiabatic limit the total current is expected to be the sum of the current contributions due to the forward and backward driving. It is readily seen from the figure, that the value of  $Pe$  in the curve for which  $T = 0.01$ , is high above  $F_0 \approx 0.72$ , i.e, when the barriers to the current(inset) in the forward direction are absent. The current steadily increases with driving until  $F_0 \approx 1.5$  where a peak in current is observed. However, beyond this value of  $F_0$ , the barriers to the motion in the other direction also disappear and hence the net current starts decreasing as can be seen from the inset of fig 7. It is notable that the value of  $Pe$  in the observed regime beyond the value of  $F_0 \approx 0.72$  is  $\gg 2$  and in fact seen to be as high as 16. In the region  $F_0 < 0.72$ , where the current in the low  $T$  limit vanishes, the transport is incoherent. For  $T = 0.1$ , the particles can take the aid of significant thermal fluctuations to cross the barriers in both directions. Hence, the current values at  $T = 0.1$  for  $F_0 > 0.72$  are much lower than those observed

for  $T = 0.01$ . Therefore, the associated  $Pe$  values are much lower for  $T = 0.1$  and the transport is seen to be completely unreliable in fig. 7.

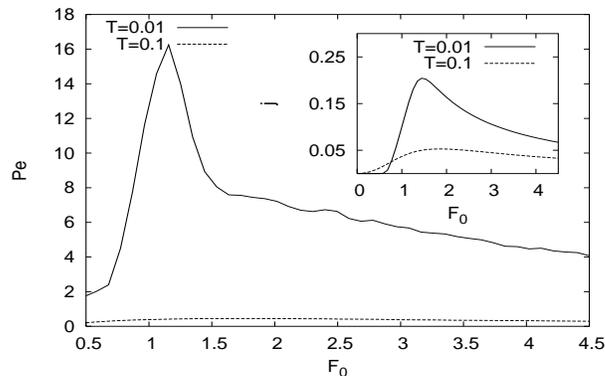


**Figure 7.** Plot of  $Pe$  and  $j$ (inset) versus  $F_0$  at  $T = 0.01$  and  $T = 0.1$  in the temporally asymmetric driving case for  $\omega = 0.25$ (adiabatic limit).

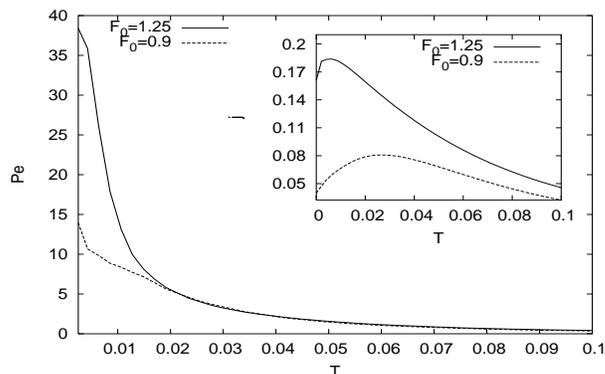


**Figure 8.** Plot of  $Pe$  and  $j$ (inset) versus  $T$  at  $F_0 = 0.9$  and  $F_0 = 1.25$  in the temporally asymmetric driving case for  $\omega = 0.25$ (adiabatic limit).

In fig. 8 we plot the variation of  $Pe$  and  $j$  (inset) as a function of  $T$  at two fixed values of  $F_0 = 0.9$  and  $F_0 = 1.25$ . We have restricted ourselves to the adiabatic( $\omega = 0.25$ ) domain of operation, where the values of  $j$  and  $Pe$  are expected to be large. For these values of  $F_0$ , a finite current results at  $T = 0$ , as shown in the inset of fig. 8. Hence, giant coherence is expected at low temperatures. To avoid divergence of  $Pe$ , the origin of the  $T$  axis is chosen at  $T = 0.0025$ . With increase in  $T$ , the transport coherence diminishes.

In fig. 9, we have plotted  $j$ ,  $D$  and  $Pe$  as a function of  $T$  for various frequencies mentioned in fig 9 at  $F_0 = 0.5$ . Fig. 9(a) reproduces the currents of fig. 1(b) of Ref. [29]. In the adiabatic limit ( $\omega = 0.25$ ), current remains positive and exhibits a peak. Current in the non-adiabatic limit ( $\omega = 4.0$  and  $\omega = 7.0$ ) starts with a negative value and exhibits current reversals [29, 40].  $D$  saturates to a value  $D/D_0 \approx 1$  in the high temperature limit. Depending on the temperature regime, whether  $D$  is a monotonic

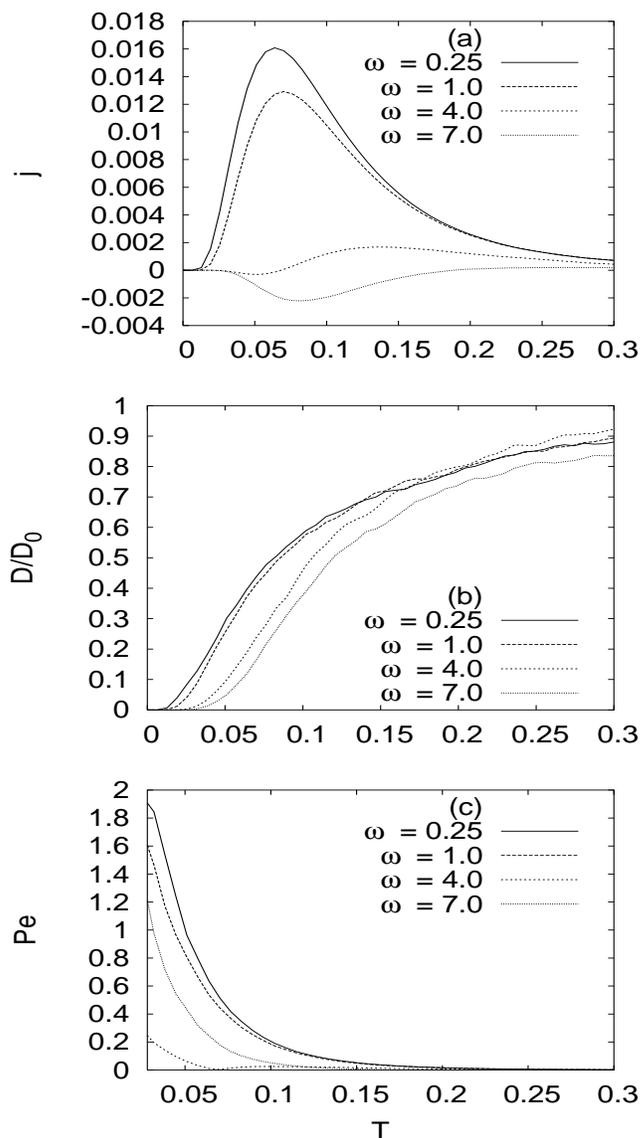


**Figure 9.** Plot of (a)  $j$  (b)  $D$  and (c)  $Pe$  (from above) versus  $T$  at  $F_0 = 0.5$  for the temporally symmetric driving case.

or non-monotonic function of frequency can be inferred from fig. 9(b). Corresponding  $Pe$  are plotted in fig 9(c). Similar to the behaviour seen in fig. 6(c), we observe that as we go from the adiabatic to the non-adiabatic regime, transport becomes incoherent. Beyond  $T = 0.1$ , the transport becomes completely unreliable ( $Pe \ll 2$ ).

## 5. Conclusions

We have studied the Brownian dynamics of a particle in a symmetric sinusoidal potential in presence of time-symmetric unbiased forcing. We have shown that the resulting fluctuation induced currents exhibit giant coherence in transport. This is observed in the parameter space where currents are finite in the deterministic limit. Moreover,

this coherence can be sustained over a large temperature range and variations in other relevant physical parameters. Transport is most coherent in the adiabatic limit and decreases as we approach the non-adiabatic limit. The coherence in transport reduces as a function of temperature and is a non-monotonic function of the amplitude of driving.

In general, the ratchet systems which favour currents in the forward direction and suppresses currents in the backward direction are expected to show enhanced coherence, other examples being flashing ratchets where two periodic states are displaced with respect to each other [11]. The ratchet systems at finite driving frequencies studied in this work exhibit several complex features in the nature of current and diffusion coefficient in the deterministic limit. Current exhibits quantisation (plateaus) associated with phase or frequency locking behaviour as a function of the amplitude of the driving force and other parameters [29, 40, 41, 42]. Correspondingly, diffusion exhibits giant peaks and crests in presence of small noise. These curves develop oscillatory features (namely resonances and antiresonances) in the presence of small noise (multiple peaks in diffusion and currents can be observed). These intriguing features can be attributed to the complex dynamics of the particle which arises due to the combined effects between non-linearity, frequency of driving and noise [42]. However, all of these complex features are not robust in the presence of finite noise, the subject matter of which is under study vis-a-vis the coherence in transport.

## Acknowledgement

One of the authors(AMJ) thanks M.C. Mahato for useful discussion and helpful suggestions.

## References

- [1] P. Reimann, Phys. Rep. **361**, 57 (2002).
- [2] F. Jülicher, A. Ajdari and J. Prost, Rev. Mod. Phys. **69**, 1269 (1997).
- [3] Special issue on “Ratchets and Brownian motors: basics, experiments and applications” ed. H. Linke, Appl. Phys. A **75** (2002)
- [4] A. M. Jayannavar, Frontiers in Condensed Matter Physics, 215, ed. J. K. Bhattacharjee and B. K. Chakrabarti, Allied Publishers(2005), India / cond-mat 0107079; D. Dan, Ph. D. thesis, 2004 (unpublished)
- [5] R. Krishnan and A. M. Jayannavar, Natl. Acad. Sci. Lett., **27**, 301(2004)
- [6] M. O. Magnasco, Phys. Rev. Lett. **71**, 1477 (1993).
- [7] M. C. Mahato, T. P. Pareek and A. M. Jayannavar, Int. J. Mod. Phys. B **10**, 3857 (1996)
- [8] K Sekimoto, 1997 J. Phys. Soc. Japan 66 6335
- [9] J. M. R. Parrondo and B. J. De Cisneros, Appl. Phys. A **75**, 179 (2002).
- [10] R. Krishnan, S. Roy and A. M. Jayannavar, J. Stat. Mech. (2005) P04012 ; R. Krishnan, M. C. Mahato and A. M. Jayannavar, Phys. Rev. E **70**, 021102 (2004)
- [11] Yu. A. Makhnovskii, V. M. Rozenbaum, D. Y. Yang , S. H. Lin and T. Y. Tsong, Phys. Rev. E **69**, 021102 (2004).
- [12] I. Derenyi, M. Bier and R.D. Astumian, Phys. Rev. Lett. , **83**, 903(1999)

- [13] D. Suzuki and T. Munakata, Phys. Rev. E, **68**, 021906(2003)
- [14] J. A. Freund and L. Schimansky-Geier, Phys. Rev. **E60**, 1304 (1999); T. Harms and R. Lipowsky, Phys. Rev. Lett. **79**, 2895 (1997).
- [15] B. Lindner and L. Schimansky-Geier, Phys. Rev. Lett. **89**, 230602 (2002).
- [16] L. Machura, M. Kostur, P. Talkner, J. Luczka, F. Marchesoni, and P. Hänggi, Phys. Rev. E **70**, 061105 (2004); L. Machura, M. Kostur, F. Marchesoni, P. Talkner, P. Hänggi and J. Luczka, J. Phys. Condens. Matter, **17**, S3741-S3752(2005)
- [17] M. J. Schnitzer and S. M. Block, Nature (London) **388**, 386 (1997); K. Visscher et al, Nature **400**, 184 (1999).
- [18] H.Y. Wang and J.D. Bao, Physica A (2006) [in press]
- [19] R. Krishnan, D. Dan and A. M. Jayannavar, Ind. J. Phys. **78**, 747 (2004); Physica A **354** 171(2005); Mod. Phys. Lett. B **19**, 971(2005)
- [20] D. R. Chialvo, M. M. Millonas, Phys. Lett. A **209**, 26 (1995).
- [21] M. C. Mahato and A. M. Jayannavar, Phys. Lett. A **209**, 21 (1995)
- [22] A. Ajdari, D. Mukamel, L. Peliti and J. Prost, J. Phys. I (France) **4**, 1551 (1994)
- [23] J. Luczka, R. Bartussek and P. Hänggi, Europhys. Lett. **31** 431 (1995)
- [24] F. Marchesoni, 1986 Phys. Lett. A **119** 221
- [25] S. Savel'ev, F. Marchesoni, P. Hänggi and F. Nori, Europhys. Lett. **67** 179(2004); Phys. Rev. E **70** 066109(2004); Eur. Phys. J. B **40** 403(2004)
- [26] R. Chacon and R. Quintero, Preprint physics/0503125 and references therein
- [27] G. M. Shmelev, N. H. Song and G. I. Tsurkan, Sov. Phys. J. (USA) **28** 161(1985); M. V. Entin, Sov. Phys. Semicond. **23** 664(1989); R. Atanasov, A. Haché, J. L. P. Hughes, H. M. vanDriel and J. E. Sipe, Phys. Rev. Lett. **76** 1703(1996); A. Haché, Y. Kostoulas, R. Atanasov, J. L. P. Hughes, J. E. Sipe and H. M. van Driel, Phys. Rev. Lett. **78** 306(1997); K. N. Alekseev, M. V. Erementchouk and F. V. Kusmartsev, Europhys. Lett. **47** 595(1999)
- [28] M. Schiavoni, L. Sanchez-Palencia, F. Renzoni and G. Grynberg, Phys. Rev. Lett. **90** 094101(2003) and references therein; P. H. Jones, M. Goonasekera and F. Renzoni, Phys. Rev. Lett. **93** 073904(2004); R. Gommers, P. Douglas, S. Bergamini, M. Goonasekera, P.H. Jones and F. Renzoni, Phys. Rev. Lett. **94** 143001(2005); R. Gommers, S. Denisov, and F. Renzoni, Phys. Rev. Lett. **96** 240604 (2006)
- [29] R. Bartussek, P. Hanggi and J.G. Kissner, Europhys. Lett. **28** 459 (1994)
- [30] H. Kamegawa, T. Hondou and F. Takagi, Phys. Rev. Lett. **80**, 5251 (1998); F. Takagi and T. Hondou, Phys. Rev. E **60**, 4954 (1999); K. Sumithra and T. Sintes, Physica A, **297**, 1 (2001); D. Dan and A. M. Jayannavar, Phys. Rev. E **65**, 037105(2002); D. Dan, M.C. Mahato and A. M. Jayannavar, Int. J. Mod. Phys., **14**, 1585(2000); D. Dan, M.C. Mahato and A. M. Jayannavar, Physica A, **296**, 375(2001)
- [31] H. Risken, The Fokker-Planck Equation (Springer Verlag, Berlin, 1984).
- [32] T. Harada, K. Yoshikawa, Phys. Rev. E **69**, 031113(2004)
- [33] M. San Miguel and R. Toral, Instabilities and nonequilibrium structures VI (Kluwer Academic, 2000)
- [34] W. H. Press, S.A. Teukolsky, W.T. Vetterling, B.P. Flannery, Numerical Recipes in C (Cambridge University Press, 1992)
- [35] H. Gang, A. Daffertshofer, H. Haken, Phys. Rev. Lett. **76**, 4874 (1996)
- [36] P. Reimann, C. Van den Broeck, H. Linke, P. Hänggi, J. M. Rubi and A. Pérez-Madrid, Phys. Rev. Lett. **87**,10602 (2001); Phys. Rev. E **65**, 031104 (2002)
- [37] D. Dan and A. M. Jayannavar, Phys. Rev. E **66**, 041106 (2002).
- [38] M. Schreier, P. Reimann, P. Hänggi and E. Pollak , Europhys. Lett. **44** 416 (1998)
- [39] R. Krishnan, J. Chacko, M. Sahoo, and A.M. Jayannavar, J. Stat. Mech. (2006) P06017
- [40] D. Dan, M.C. Mahato and A. M. Jayannavar, Phys. Rev. E **63**, 056307 (2001)
- [41] D. Dan, G. I. Menon and A. M. Jayannavar, Physica A, **318** 40(2003)
- [42] D. Reguera, P. Reimann, P. Hänggi and J.M. Rubi, Europhys. Lett. **57** 644 (2002)